Ceramics-Silikáty 67 (4), 411-419 (2023)
www.ceramics-silikaty.cz doi: 10.13168/cs.2023.0041

ANTIOXIDANT AND ANTI-TUMOUR ACTIVITIES OF INULA VISCOSA L EXTRACT-LOADED NANOFIBROUS MATS FOR BIOMEDICAL APPLICATIONS

SUMEYYE CESUR

Center for Nanotechnology & Biomaterials Application and Research (NBUAM), Marmara University, Turkey
Department of Metallurgical and Materials Engineering, Faculty of Technology, Marmara University, Turkey

#E-mail: sumeyye.cesur@marmara.edu.tr, sumeyye-cesur@hotmail.com

Submitted August 8, 2023; accepted September 12, 2023

Keywords: Electrospinning, Antioxidant activity, Anti-tumour activity, Polylactic acid, Polyethylene glycol, Inula viscosa (L.)

Plants have been used for medicinal purposes for thousands of years. Knowledge of traditional medicine has encouraged the further exploration of medicinal plants as potential drugs. Therefore, in this study, IVE-loaded PLA/PEG nanofibrous mats were successfully produced by the electrospinning method. When the SEM images were analysed, it was seen that nanofibrous patches with a smooth surface were acquired in both the pure and IVE-loaded nanofibrous mats. A significant reduction in the mean fibre diameters was seen with the implication of the plant extract. Based on the FT-IR and DSC studies, it was proven that the IVE is fully incorporated into the PLA/PEG nanofibrous mats. In the tensile test results, it was observed that the addition of the IVE to the PLA/PEG combination increased the tensile strength. Considering the antioxidant activity results, it was observed that while the PLA/PEG did not show any antioxidant effect, the antioxidant activity increased with the concentration of the IVE ratio in the nanofibrous mats. Based on the in vitro tests using HCT-116 colon cancer cells, the IVE dramatically and dose-dependently reduced the cell proliferation in the tested cancer cell lines. When all the results are evaluated, it is thought that IVE-loaded nanofibrous mats can be a new and effective treatment against the disease in biomedical applications.

INTRODUCTION

Since ancient times, natural remedies have been utilised to heal a variety of illnesses. Growing interest has been shown in the utilisation of medicinal herbs as potent candidates for new anticancer treatment medicines due to their extensive use in traditional medicine. [1, 2]. Phenolic compounds as secondary metabolites with a polyphenol hydroxy configuration are typically found in plants [3]. Natural phenolic compounds, which are widely employed in medicine and pharmaceuticals for the prevention and treatment of major diseases, have received increased attention in recent years [4]. The most important classes of natural antioxidants are phenolic compounds, which are significant sources of antioxidant activity [5]. The biochemical components of the human body are protected against oxidative stress by phenolic substances obtained from plants. On the other side, disease-related situations lead to oxidative stress, which harms cells. Although synthetic substances can reduce oxidative damage, they also come with drawbacks over prescription drugs. Herbal extracts have a number of advantages, they have fewer negative effects, are less expensive, easier to produce and handle, more accessible, and more effective [6]. Some plant extracts contain antihyperlipidemic, antioxidant, antitumour, and anti-inflammatory properties [7].

Inula viscosa (L.) (IV), a popular medicinal plant in the Asteraceae family is aiton. It has a long history of usage as a treatment for infertility, cancer, bronchitis, diabetes, gastroduodenal issues, skin conditions, rheumatoid arthritis, and lung ailments. Inula viscosa (L.) extract (IVE) has been shown to have antioxidant, antibacterial, anticancer, cytotoxic, antihypertensive, hypoglycaemic, hypolipidemic, abortifacient, and anti-implantation actions in earlier research [8–10]. However, in the literature search, a few studies were conducted on the IV nanofibre structure [11]. Numerous investigations have indicated the existence of various physiologically active substances in IV and their ability to cause

apoptosis in cancer cells, including polyphenols [12] and sesquiterpenes. Danino et al. [13] extracted polyphenolic antioxidants from IV leaves, including seven derivatives from the caffeoylquinic acid (CQA) and dicaffeoylquinic acid (diCQA) families. These chemicals may have synergistic effects in the treatment of cancer. This premise, combined with the need for novel colon cancer therapy options, motivates us to investigate the anti-carcinogenic effects of IV leaf water extract on colon cancer cell development in vitro and in vivo, as well as to determine the mechanism of action [14].

In order to maintain the qualities of plant-derived products, they can be encapsulated to increase their bioavailability. It is conceivable to encapsulate antioxidant chemicals in polymeric or non-polymeric matrices thanks to nanotechnologies and microtechnologies [15, 16]. Thus, research has developed into investigating the potential properties and uses of plant extracts for the preparation of potential nanomaterial-based drugs for diseases. The manufacture of continuous non-woven nano- or microfibres with an adjustable diameter utilising a capillary through which a polymer solution is pumped while being subjected to a high-voltage source and a collector is one of the nanotechnology applications that is generating increasing interest. In ecologically friendly applications, polylactic acid (PLA), a kind of green semi-crystalline polyester made from renewable resources, offers greater advantages than petroleum-based polymers that are not biodegradable due to its biodegradability and biocompatibility. However, poor flexibility, high brittleness, and poor mechanical qualities are drawbacks of PLA nanofibres [17]. Therefore, it is critical to enhance the PLA nanofibre's mechanical attributes for applications in the future. Polyethylene glycol (PEG) shows great promise as a plasticising agent for PLA as it provides a large enhancement in the elongation at break [18,19] For biomedical, biotechnological, and pharmaceutical applications, PEG is frequently used as a reference polymer due to its great biocompatibility, non-toxicity [20], and simplicity of eliminating it from the human body [21]. Drug-loaded PLA-PEG nanofibrous mats have been prepared and studied in recent years, and their use as antibacterial wound dressings has been documented [22]. Also, the antioxidant activity of extract-loaded nanofibrous mats was identified in our previous study [23].

In this study, nanofibrous mats with both antioxidant and anticancer properties were obtained by adding IVE to PLA/PEG at different rates by the electrospinning method. The morphology of the nanofibrous mats, scanning electron microscopy (SEM), thermal properties, differential scanning calorimetry (DSC), different functional groups, and bond structures were evaluated by Fourier transform infrared (FT-IR) spectroscopy. In addition, the mechanical properties, antioxidant activity, and anticancer effects of HCT116, a colon cancer cell, of nanofibrous mats were investigated.

EXPERIMENTAL

Materials

Polyethylene glycol 4000 (PEG 4000), Mw ¼ 3500 – 4500 $g \cdot mol^{-1}$, was obtained from Sigma Aldrich. The polylactic acid (PLA) 2003D was purchased from Nature Works LLC, Minnetonka, MN, USA. The acetic acid (CH_3COOH), Tween 80 (viscous liquid), Chloroform, Citric acid, 1,1-Diphenyl-2-picrylhydrazyl radical (DPPH); 6-hydroxy-2,5,7,8-tetramethylchroman-2-carboxylic acid (Trolox); Trolox (6-hydroxy-2,5,7,8-tetramethylchroman-2-carboxylic acid), Folin-Ciocalteu phenol reagent, gallic acid (GA), sodium carbonate, 2,4,6-tri(2-pyridyl)-s-triazine (TPTZ), PBS (phosphate-buffered saline) pH 7.4 solution were obtained from Sigma Aldrich. The HCT 116 Cell Line Human, DMEM high glucose with 4.5 $g \cdot L^{-1}$ d-glucose was bought from Sigma-Aldrich (St. Louis, MO, USA).

Preparation of solvent extracts

In 2021, the root pieces of the IV plant were taken from the Manisa Akhisar province in Kasm. The dried material was processed into a fine powder in a blender. A total of 2 g of pulverised sample was weighed. The sample was extracted in three phases with 25 mL of solvent for 60 minutes, 25 mL for 60 minutes, and 25 mL for 60 minutes in an ultrasonic bath, orbital shaker, and heated magnetic stirrer at 60 °C in a closed glass shot bottle. These three extracts were mixed to form a 30 ml solution. As the solvents, water, and ethanol (70 %) were utilised. After extraction, the extracts were centrifuged for 20 minutes at 2500 rpm. The supernatant was separated and kept at -20 °C until the analysis was performed. The dried material was processed into a fine powder in a blender. Two grams (2 g) of powdered IV roots were then extracted in an ultrasonic extraction apparatus for 1 hour and three consecutive extractions at 60 °C with 70 % ethanol were performed. The extract was dried in an evaporator at 50 °C under reduced pressure after being filtered through Whatman blue band filter paper. The final residue (crude extracts) was measured and kept in bottles at +4 °C. In order to test for nanofibre production, the unprocessed extracts were dissolved in DMSO.

Preparation of electrospinning solutions

PLA was dissolved in chloroform for about 90 minutes with magnetic stirring (IKA, RCT, Germany) to achieve an 8 wt. % concentration at room temperature. After that, 3 wt. % Tween 80 was added to the PLA solution and stirred for another 15 minutes. After mixing, 1 % PEG was added to the solution, which was then agitated for 10 minutes [24]. To make solutions with the IVE plant extract, IVE solutions in ethanol (70:30, v/v) at diverse concentrations (20 mg, 40 mg, and 60 mg) were added to the PLA/PEG blend and swirled for 20 minutes independently.

Fabrication of Electrospun Nanofibrous Mats

The electrospinning technique was used to create the nanofibrous mats (Figure 1). A syringe pump (NE-300, New Era Pump Systems, Inc. USA), a single brass needle (diameter 1.63 mm), a high voltage power source attached to the needle, and an electrospinning machine (NS24, Inovenso Co. Turkey) comprise the experimental set-up. The homogeneous spinning solutions were poured into disposable syringes with a volume of 10 ml. Using a syringe pump, the solutions were given at a steady flow rate of 2 ml·h^{-1} for electrospinning at 18 kV. The operating distance was set to 120 mm from the needle tip to the oily paper-coated circular collector. All the investigations were carried out at room temperature (25 °C) [25].

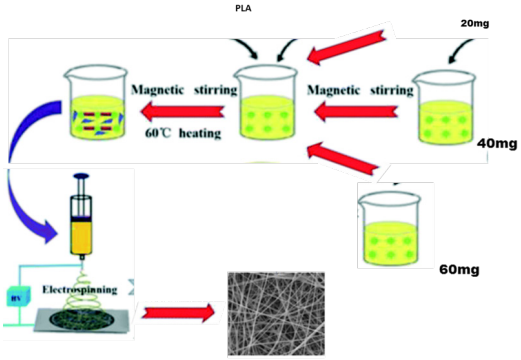

Figure 1. Schematic representation of the electrospinning process.

Characterisation of the Nanofibrous Mats

Scanning electron microscopy

The morphology of the nanofibrous mats was examined using a scanning electron microscope (SEM) (EVO LS 10, ZEISS) after 120 seconds of gold-palladium coating. The accelerating voltage used was 10 kV. The diameters of the nanofibrous mats were measured using image analysis software (Olympus AnalySIS, USA), which randomly selected 100 nanofibrous mats from each SEM picture. The data were imported into the SPSS software for additional analysis.

Fourier transform infrared (FTIR) spectroscopy

The functional groups of the nanofibrous mats were qualitatively characterised using a Fourier-transformed infrared (FTIR) spectroscopy analysis (Jasco FT/ IR-4700). Each spectrum was captured between 4000 and 400 cm^{-1} and averaged across 32 scans at a resolution of 4 cm^{-1}.

Differential scanning calorimetry (DSC)

The thermal properties of the nanofibrous mats, such as the melting temperatures (T_m) and glass transition temperatures (T_g), were measured using a differential scanning calorimeter (DSC) (Shimadzu, Japan). All the nanofibrous mat groups had their temperature ranges changed to range from 25 to 300 °C (scanning rate: 10 C·min^{-1}).

Mechanical Properties

Before starting the test, each sample was cut to 5 cm long and 1 cm wide, and the thickness of the various types of nanofibrous mats was measured with a digital micrometer (Mitutoyo MTI Corp. USA). A tensile testing equipment (Shimadzu Corporation, EZ-LX, Kyoto, Japan) was used to evaluate the mechanical properties. Three distinct samples were examined for each group.

Total phenolic content

The Folin Ciocalteu (FCR) method was used to determine the total polyphenol content of the IVE-loaded nanofibres [16]. Nanofibrous mats (0.01 g) were extracted for the first hour in an orbital shaker incubator (BIOSAN ES-20) at a constant stirring speed (200 rpm, 37 °C) with 70 % ethanol (v/v). In a nutshell, 100 µl of each sample was combined with 4 ml of water and 100 µl of the Folin-Ciocalteu reagent. Each sample was then treated with 100 µl of sodium carbonate (6 %). After 30 minutes of processing, the absorbance was measured between 685-760 nm using a spectrophotometer (Shimadzu UV-1601, Japan). The calibration curve was created using a gallic acid standard at concentrations ranging from 62.5 to 1000 µM (y = 0.0018 x-0.0079, R^2 = 0.9998). The results were represented in gallic acid equivalents per millilitre (GAE/ml). Every measurement was taken three times.

Determination of the radical scavenging ability by using DPPH method

Ayaz Seyhan [26] examined the 2,2-diphenyl-1-picrylhydrazyl (DPPH) radical scavenging activity of the IVE-loaded nanofibrous mats. In brief, 1.5 mL of each sample was mixed with 1.5 mL of the DPPH radical solution (100 µM) and incubated for 30 minutes in an orbital shaker-incubator (BIOSAN ES-20) at a constant stirring speed (200 rpm, 37 °C). A spectrophotometer (Shimadzu UV-1601, Japan) was used to detect the absorbance at 515-528 nm. The calibration curve was created using the Trolox standard at concentrations ranging from 62.5 to 1000 µM (y = 0.00106 + 0.0620 R^2 = 0.9932). Trolox equivalents (TE/ml) were used to express the results. Each measurement was taken three times.

Cell Viability Analysis

Fibrous patches were cut into 6 mm diameter discs for the cell viability analysis and sterilised on both sides under UV light. Before cell seeding, the nanofibrous mats were then cultured in a cell culture medium for

4 hours. In a 37 °C incubator with 5 % CO_2 humidified air, HCT-166 cells were grown in Dulbecco's modified Eagle medium (DMEM, Gibco) containing 10 % foetal bovine serum (FBS, Gibco) and 1 % penicillin/streptomycin. At the same time, monolayer (2D) cell cultures were incubated as a control group. The cell viability was analysed by [3-(4,5-dimethylthiazol-2-yl)-2,5-diphenyltetrazolium bromide] (MTT) analysis after 1, 3 and 7 days of incubation. The samples were first washed with pH 7.4 PBS and then 0.5 mg·mL^{-1} (0.5 mL) of the MTT solution was added. After incubation at 37 °C with 5 % CO_2 for 3 hours, the supernatant was removed and 1.5 mL of dimethylsulfoxide (DMSO) was added to it, according to the manufacturer's protocol. After incubation for 15 minutes, the absorbance values were measured with a microplate reader (Enspire, Perkin Elmer) at a 550 nm wavelength.

Statistical analysis

The data received from the measurements were statistically analysed using a single-factor analysis of variance (ANOVA) analytic tool. The SPSS analytical tool was used to measure the diameters of the nanofibres. All the results are reported as the mean standard deviation. The statistical significance level was set at $p < 0.05$.

RESULTS AND DISCUSSION

Morphology of the nanofibrous mats

SEM was used to examine the surface morphology of the nanofibrous mats. Based on the SEM images of the nanofibres, 100 random diameter measurements were taken for each sample to construct the diameter distribution graphs. Figure 2 shows the SEM images as the well as diameter distribution histograms. The surface morphologies of the non-extracted and extract-loaded nanofibre patches were highly homogeneous and smooth, with no apparent beads. The mean nanofibrous mat diameter of the PLA/PEG nanofibrous mats was determined as ϕ = 1681.14 ± 530.918 nm (Figure 2). A significant thinning of the mean fibre diameters was experienced with the inclusion of the plant extract. The average fibre diameters of the extract-loaded nanofibrous mats were measured as ϕ = 671.62 ± 173.355 nm for the PLA/PEG/20mg IVE, ϕ = 633.62 ± 173.355 nm for the PLA/PEG/40mg IVE, and ϕ = 541.75 ± 122.979 nm for the PLA/PEG/60mg IVE. Consequently, the plant extract-loaded nanofibrous mats demonstrated smaller diameters which were compared to the PLA/PEG nanofibrous mats. A similar observation was reported by [25]. In addition, it was observed that the fibre diameter gradually decreased as the amount of extract increased. Sriyanti et al. loaded three different ratios of plant extracts into the PVA solution and found the same result [27]. Likewise, Yousefi et al. loaded a chitosan-based solution with three different extracts and observed that the fibre diameter decreased with an increasing extract amount [28].

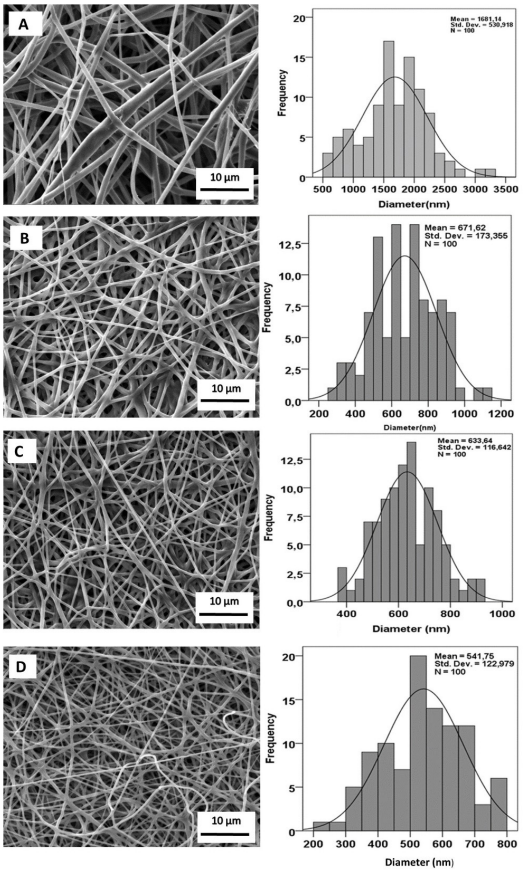

Figure 2. SEM images and fibre diameter distribution of the (a) pure PLA/PEG, (b) PLA/PEG/20 IVE, (c) PLA/PEG/40 IVE, (d) PLA/PEG/60 IVE.

Chemical properties of the nanofibrous mats

An FTIR analysis was carried out to investigate the chemical structures of the nanofibrous mats. For IVE (Figure 3a), at 2925 cm^{-1}, belonging to the C–H symmetric stretching vibrations of the polyphenolic structures, the peak at 1440 cm^{-1} can also be formed by the contribution of aromatic C=C bonds [29]. The peak in the range of 927 cm^{-1} - 750 cm^{-1} indicates the C–H out-of-plane bending vibrations of the substitute aromatic ring. Figure 3b shows the peaks of the PEG. C–H stretching is observed at 2890 cm^{-1} and, at the peak 1125 cm−1, C–O (ether) stretching can be seen [24]. In Figure 3c, absorption peaks for the PLA are shown. The peak at 1749 cm^{-1} shows the C=O vibration. The peak, which is seen at 1453 cm^{-1}, corresponds to the CH_3 asymmetrical scissoring [30]. C–CH_3 stretching is observed at the peak at 1042 cm^{-1}. The absorption peaks of the produced

nanofibrous mats are observed in Figure 3d, e, f, and g. It was observed that all of the produced nanofibrous mats in Figure 3d, e, f, g were given peaks at the same peak point of 2884 cm^{-1} which indicates the characteristic C–H alkyl stretching thus confirming the presence of PLA/PEG. Also, all the produced nanofibrous mats show a strong absorption band at 1080 cm^{-1}, which is due to the C–O–C stretching. In Figures 3e, f, g, the absorption peak commonly observed in the range of 1700 cm^{-1} - 1750 cm^{-1}, but is be visible in Figure 3d. This peak arises from the incorporation of the plant extract. This band is assigned to stretching vibrations of the C=O bonds in the carboxyl group. All the produced nanofibrous mats with IVE shown in Figure 3e, f, and g showed C=O stretching vibrations at 1591 cm^{-1}, 1598 cm^{-1}, and 1595 cm^{-1}, respectively. Small shifts at this absorption peak may result from the conjugation of the carbonyl group bonded to an aromatic ring. Conjugated C=C stretching vibrations of the aromatic ring were detected at 1600 cm^{-1} which is shown in Figure 3e, f, g.

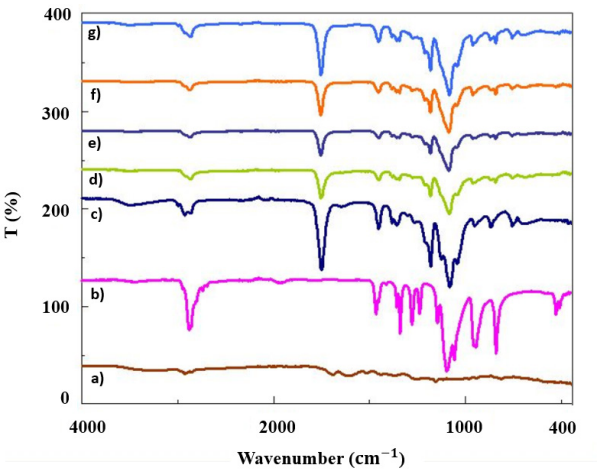

Figure 3. FTIR spectra of IVE (a), PEG (b), PLA (c), PLA/PEG (d), PLA/PEG/20 IVE (e), PLA/PEG/40 IVE (f), PLA/PEG/60 IVE (g).

is in a highly amorphous form in the pure PLA/PEG, the decreased cold-crystallinity is associated with the increase in the plant extract ratio [32]. With the addition of PEG, the mobility and flexibility of the polymer chain of the PLA positively improve. When evaluated according to the curves in the TG graphs, it is seen that the thermal stability of PLA decreases with the addition of PEG [33, 34]. The melting temperature of PLA/PEG nanofibrous mats has been observed to be 151.3 °C. This melting temperature is attributed to the presence of the PLA content [35]. With the addition of IVE to the PLA/PEG nanofibrous mats, the melting temperatures for PLA/PEG/20 IVE, PLA/PEG/40 IVE, PLA/PEG/60 IVE were determined as 155.5 °C, 159.0 °C, and 153.7 °C, respectively. It is hypothesised that these small shifts in melting temperature may be caused by the addition of IVE to the PLA/PEG nanofibrous mats. It was determined that the thermal stability of the composites formed by the addition of extract to PLA/PEG mixtures increased. Taking all the DSC data into account, loading the IVE to PLA/PEG nanofibrous mats affected the mobility of the molecular chains and altered the way the material behaved thermally. This output is found to be in good accordance with the experimental findings from studies on the nanofibrous mat morphology and mechanics.

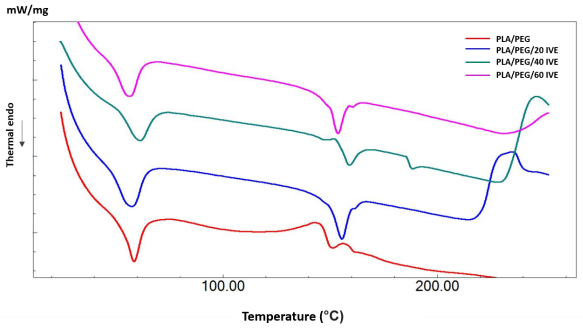

Figure 3. DSC thermogram of the pure PLA/PEG and IVE-loaded nanofibrous mats in three different concentrations (20, 40, and 60 mg).

Thermal properties of the nanofibrous mats

Thermal characterisation techniques play a crucial role in determining the chemical and physical changes within a material's molecular structure, including the glass transition temperature (T_g) and melting temperature (T_m) [31]. A DSC analysis was applied to evaluate the thermal properties of the nanofibrous mats, and the resultant thermograms obtained for PLA/PEG, PLA/PEG/20 IVE, PLA/PEG/40 IVE, and PLA/PEG/60 IVE are shown in Figure 4. The glass transition temperatures for PLA/PEG, PLA/PEG/20 IVE, PLA/PEG/40 IVE, PLA/PEG/60 IVE nanofibrous mats were 58.6 °C, 57.6 °C, 61.4 °C and 56.4 °C, respectively. The DSC results indicate that while cold-crystallisation

Mechanical Properties

The mechanical characteristics of nanofibrous mats vary depending on a variety of conditions, and these qualities are critical in identifying nanofibre applications. Material selection has a significant impact on the mechanical properties of the generated nanofibres [36]. Figure 5 shows the tensile properties of all the nanofibre patches at room temperature, with values of tensile strength and elongation at break (%). The PLA/PEG nanofibrous mats presented a tensile strength of 1.20 ± 0.23 MPa and a strain at a break of 103.64 ± 7.1. When the extracts were loaded onto these PLA/PEG

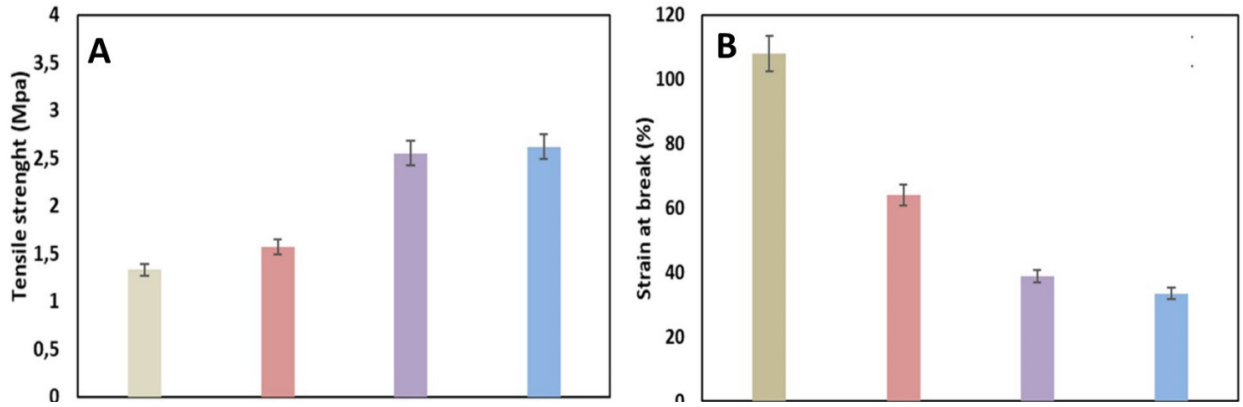

Figure 5. Physical parameters of the nanofibrous mats: (A) tensile strength and (B) strain at break.

nanofibrous mats, their tensile strength gradually increased, reaching 2.81 ± 0.35 MPa. The strain at break also decreased, conversely, to 51.61 ± 21.1 %. As can be seen, the mechanical characteristics of the nanofibres improved with the addition of the extract. The tensile strength value increased, while the strain at break value decreased lightly after the addition of the 20 mg (PLA/PEG/20 IVE) extract to the polymer matrix. The tensile strength and strain at the break values improved as the extracted content was increased to 60 mg (PLA/PEG/60 IVE) [37]. In addition, Al-Kaabi et al. observed that the mechanical properties increased as the extract was added to the polymer matrix [38]. These findings are consistent with the literature. As seen in Figure 2, this observation can be explained by the changes in fibre diameter and dispersion. When the extract concentration was increased, the diameter and dispersion of the fibres decreased. As a result, the fibre with a smaller diameter demonstrated superior mechanical qualities.

Phenolic content and antioxidant properties

The total phenolic content of the IVE-loaded nanofibrous mats was evaluated using the Folin-Ciocalteu reagent, and the nanofibres' free radical scavenging activity was determined using the DPPH radical. Figure 6 shows that PLA/PEG nanofibrous mats have a very low DPPH, while the PLA/PEG/IVE nanofibrous mats exhibit significant antioxidant activity and lowering capability. This suggests that high voltage exposure during the electrospinning process has no effect on the antioxidant activity. The pure PLA/PEG nanofibrous mats, as expected, had no antioxidant impact; rather, they acted as a reservoir and protection mechanism for the antioxidants discovered in the studied IVE [39].

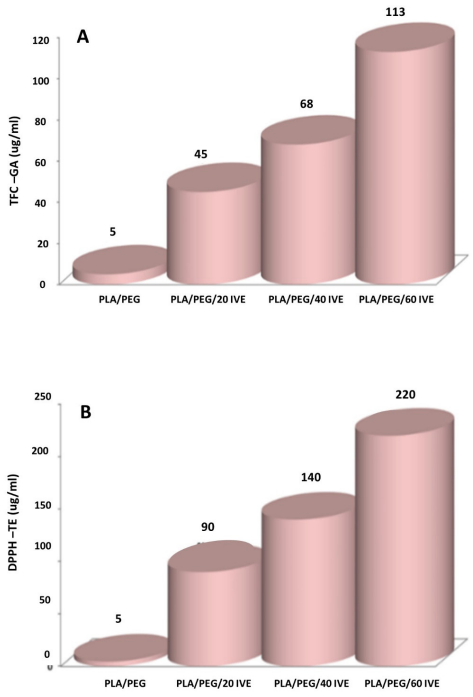

Figure 6. Total phenolic contents and antioxidant activity of the nanofibrous mats: A) Folin-Ciocalteu B) DPPH .

In vitro Cytotoxicity

The effects of the IVE-loaded and unloaded nanofibrous mats on the cell viability were examined by MTT analysis for 1, 3, and 7 days. HCT-116 colon cancer cell lines were used in the MTT analysis of the produced nanofibrous mats and the results are demonstrated in Figure 7. Compared to the 2D control, the effects of pure PLA/PEG nanofibrous mats without IVE on the cell viability were in the range of 80 % - 90 % in the 1st, 3rd, and 7th day MTT analyses. Although the pure group has a slight lethality on cancer HCT-116 colon cancer cells, it is not a significant rate. However, the lethality of PLA/PEG/20 IVE nanofibrous mats on HCT-116 colon cancer cells was calculated as 26.4 %, 25.1 %, and 22 % on days 1, 3, and 7, respectively. Similar results were obtained with 10.3 %, 10.1 %, and 10.3 % for PLA/PEG/40IVE nanofibrous mats and 7.2 %, 8.7 %, and 9.9 % for PLA/PEG/60IVE nanofibrous mats, respectively. When the results are examined, the addition of IVE to the nanofibres has a positive effect on killing cancer cells. After 1, 3 and 7 days of incubation, it can be said that the viability of the cells decreased more. The decrease in the cell viability as the incubation time increased may be related to the increase in the amount of IVE released into the medium day by day. In addition, it can be observed from the results that the increasing amount of IVE in the nanofibrous mats decreases the viability of HCT-116 cancer cells. In conclusion, increasing the amount of IVE in the medium increased the toxicity for HCT-116 colon cancer cells. Merghoub et al. investigated the antiproliferative effect of IVE on different cancer cell lines by performing an MTT analysis. According to the results, IVE significantly inhibited cell growth in the tested cancer cell lines in a dose-dependent manner [40]. In another study, Virdis et al. investigated the adverse effects of IVE extract on Raji cancer cells. Increasing IVE ratios from 10 $\mu g \cdot ml^{-1}$ to 80 $\mu g \cdot ml^{-1}$ increased the cell apoptosis, showing a proportional decrease in the cell viability [41]. When the results are compared with the literature, the increased lethal effect of IVE amount and incubation time on HCT-116 colon cancer cells is supported by the literature.

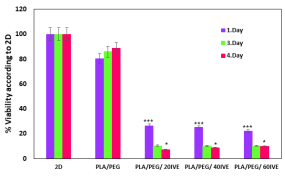

Figure 7. . Cell viability results of the nanofibres for 1-day, 3-day, and 7-day incubation. 2D was accepted as a control. One-way Analysis of Variance (ANOVA) Tukey-Kramer Multiple Comparisons Test comparison to 2D, **p < 0,01, ***p < 0,001.

CONCLUSIONS

In this study, PLA/PEG nanofibrous mats loaded with IVE were successfully produced by the electrospinning method. Among synthetic polymers, PLA/PEG, as a copolymer, has been particularly chosen as a drug delivery system, often for various types of cancer. An IVE plant extract, whose antioxidant and anticancer effect has been proven in the literature, was added to the nanofibrous mats at different concentrations. When the SEM images were analysed, it was seen that fibrous patches with smooth and bead-free surfaces were obtained in both the pure and IVE-loaded nanofibrous mats. A significant reduction in the mean fibre diameters was seen with the inclusion of the plant extract. Based on the FT-IR and DSC studies, it has been proven that IVE is fully incorporated into the PLA/PEG nanofibrous mats. The tensile test results showed that the addition of the extract improved the mechanical properties of the nanofibres. It was observed that the addition of IVE to the PLA/PEG combination increased its tensile strength. Considering the antioxidant activity results, it was observed that while PLA/PEG did not show any antioxidant effect, the antioxidant activity increased with the concentration of the IVE ratio in the nanofibrous mats. Based on the in vitro studies with HCT-116 colon cancer cells, the IVE significantly inhibited cell growth in the tested cancer cell lines in a dose-dependent manner. This shows that materials containing IVE showed promising antitumour activity. When all the results are evaluated, it is thought that IVE-loaded nanofibrous mats can be a new and effective treatment against the disease with a local application in biomedical applications. As it turns out, the discovery of natural product chemistry is important to identify potential new drug candidates that will help maintain health and fight disease and illness.

REFERENCES

1. Greenwell M., Rahman P.K.S.M. (2015): Medicinal Plants: Their Use in Anticancer Treatment. *International Journal of Pharmaceutical Sciences and Research, 6*, 4103–4112. doi:10.13040/IJPSR.0975-8232.6(10).4103-12
2. Dias D.A., Urban S., Roessner U. (2012): A historical overview of natural products in drug discovery. *Metabolites, 2*, 303–336. doi:10.3390/metabo2020303
3. Pereira D.M., Valentão P., Pereira J.A., Andrade P.B. (2009): Phenolics: From Chemistry to Biology. *Molecules, 14*, 2202–2211 doi:10.3390/molecules14062202
4. Yakub G., Ignatova M., Manolova N., Rashkov I., Toshkova R., Georgieva A., Markova N. (2018): Chitosan/ferulic acid-coated poly(ε-caprolactone) electrospun materials

with antioxidant, antibacterial and antitumor properties. *International Journal of Biological Macromolecules, 107*, 689–702. doi:10.1016/j.ijbiomac.2017.08.183

5. Ayaz Seyhan S., Demirel A.B., Cesur S., Bilgic Alkaya D. (2023): Production, characterization, and antioxidant activity evaluation of Rheum Ribes L. extract-loaded PLA/PEG nanofibers. *Journal of Research in Pharmacy, 27*, 146–156. doi:10.29228/jrp.299
6. Calixto J.B. (2019): The role of natural products in modern drug discovery. *Anais Da Academia Brasileira de Ciencias, 91*, 1–7. doi:10.1590/0001-3765201920190105
7. Stoyanova N., Spasova M., Manolova N., Rashkov I., Georgieva A., Toshkova R. (2020): Antioxidant and Antitumor Activities of Novel Quercetin-Loaded Electrospun Cellulose Acetate/Polyethylene Glycol Fibrous Materials. *Antioxidants, 9*, 232. doi:10.3390/antiox9030232
8. Ounaissia K. (2021): Total Phenol Content, Antioxidant And Anti-Inflammatory Activities Of Inula Viscosa From Guelma-Algeria. *International Journal of Agricultural and Natural Sciences, 14*(3), 186-193.
9. Qneibi M., Hanania M., Jaradat N., Emwas N., Radwan S. (2021): Inula viscosa (L.) Greuter, phytochemical composition, antioxidant, total phenolic content, total flavonoids content and neuroprotective effects. *European Journal of Integrative Medicine, 42*, 101291. doi:10.1016/j.eujim.2021.101291
10. El Yaagoubi O.M., Lahmadi A., Bouyahya A., Filali H., Samaki H., El Antri,S. Aboudkhil S. (2021): Antitumor Effect of Inula viscosa Extracts on DMBA-Induced Skin Carcinoma Are Mediated by Proteasome Inhibition, *BioMed Research International,* 2021, 6687589. doi:10.1155/2021/6687589
11. Moussaoui N., Rokbi M., Osmani H., Jawaid M., Atiqah A., Asim M., Benhamadouche L. (2021): Extraction and Characterization of Fiber Treatment Inula viscosa Fibers as Potential Polymer Composite Reinforcement. *Journal of Polymers and the Environment, 29*, 3779–3793. doi:10.1007/s10924-021-02147-w
12. Talib W.H., Mahasneh A.M. (2010): Antiproliferative activity of plant extracts used against cancer in traditional medicine. *Scientia Pharmaceutica, 78*, 33–45. doi:10.3797/scipharm.0912-11.
13. Danino O., Gottlieb H., Grossman S., Bergman M. (2009): Antioxidant activity of 1,3-dicaffeoylquinic acid isolated from Inula viscosa. *Food Research International, 42*, 1273–1280. doi:10.1016/j.foodres.2009.03.023
14. Bar-Shalom R., Bergman, Grossman M. S., Azzam N., Sharvit L., Fares F. (2019): Inula Viscosa Extract Inhibits Growth of Colorectal Cancer Cells in vitro and in vivo Through Induction of Apoptosis. *Frontiers in Oncology, 9,* 227. doi:10.3389/fonc.2019.00227
15. Özcan O., Erdal H., Çakırca G., Yönden Z. (2015): Oxidative stress and its impacts on intracellular lipids, proteins and DNA. *Journal of Clinical and Experimental Investigations, 6*, 331–336. doi:10.5799/ahinjs.01.2015.03.0545
16. Cikla Yilmaz D., Ayaz Seyhan S. (2017): Antioxidant Potential Of Cydonia Oblonga Leaves. *Istanbul Journal of Pharmacy, 47*, 9–11. doi:10.5152/istanbuljpharm.2017.003
17. Jahani H., Jalilian F.A., Wu C.-Y., Kaviani S., Soleimani M., Abbasi N., Ou K.-L., Hosseinkhani H. (2015): Controlled surface morphology and hydrophilicity of polycaprolactone toward selective differentiation of mesenchymal stem cells to neural like cells. *Journal of Biomedical Materials Research Part A,103*, 1875–1881. doi:10.1002/jbm.a.35328
18. Coverdale B.D.M., Gough J.E., Sampson W.W., Hoyland J.A. (2017): Use of lecithin to control fiber morphology in electrospun poly (ε-caprolactone) scaffolds for improved tissue engineering applications. *Journal of Biomedical Materials Research Part A, 105*, 2865–2874. doi:10.1002/jbm.a.36139
19. Hwang P.T.J., Murdock K., Alexander G.C., Salaam A.D., Ng J.I., Lim D.-J., Dean D., Jun H.-W. (2016): Poly(ε-caprolactone)/gelatin composite electrospun scaffolds with porous crater-like structures for tissue engineering. *Journal of Biomedical Materials Research Part A, 104*, 1017–1029. doi:10.1002/jbm.a.35614
20. Uzun Kart E. (2021): A Novel Method To Synthesis Of Calcium Sulphate Anhydrite Self-Doped With SiO_2 From Red Mud As A Bioceramic. *Ceramic-Silikaty, 65*, 344–353. doi:10.13168/cs.2021.0036
21. Cesur S., Oktar F.N., Ekren N., Kilic O., Alkaya D.B., Seyhan S.A., EgeZ .R., Lin C.-C., Kuruca S.E., Erdemir G., Gunduz O. (2019): Preparation and characterization of electrospun polylactic acid/sodium alginate/orange oyster shell composite nanofiber for biomedical application. *Journal of the Australian Ceramic Society, 56*, 533–543. doi:10.1007/s41779-019-00363-1
22. Nazari T., Moghaddam A.B., Davoodi Z. (2019): Optimized polylactic acid/polyethylene glycol (PLA/PEG) electrospun fibrous scaffold for drug delivery: effect of graphene oxide on the cefixime release mechanism. *Materials Research Express, 6,* 115351. doi:10.1088/2053-1591/ab508d
23. Seyhan S.A., Alkaya D.B., Cesur S., Sahin A. (2023): Investigation of the antitumor effect on breast cancer cells of the electrospun amygdalin-loaded poly(l-lactic acid)/poly(ethylene glycol) nanofibers. *International Journal of Biological Macromolecules, 239*, 124201. doi:10.1016/j.ijbiomac.2023.124201
24. Cesur S., Ulag S., Ozak L., Gumussoy A., Arslan S., Yilmaz B.K., Ekren N., Agirbasli M., Kalaskar D.M., Gunduz O. (2020): Production and characterization of elastomeric cardiac tissue-like patches for Myocardial Tissue Engineering. *Polymer Testing, 90*, 106613. doi:10.1016/j.polymertesting.2020.106613
25. Cam M.E., Cesur S., Taskin T., Erdemir G., Kuruca D.S., Sahin Y.M., Kabasakal L., Gunduz O. (2019): Fabrication, characterization and fibroblast proliferative activity of electrospun Achillea lycaonica-loaded nanofibrous mats. *Europen Polymer Journal, 120*, 109239. doi:10.1016/j.eurpolymj.2019.109239
26. Ayaz-Seyhan S. (2019): DPPH Antioksidan Analizinin Yeniden Değerlendirilmesi, *Batman Üniversitesi Yaşam Bilim Dergisi, 9*, 125–135.
27. Sriyanti I., Jauhari J. (2019): Electrospun of poly(vinyl alcohol) nanofiber as carrier of Garcinia mangostana L. pericarp extract. *Journal of Physics: Conference Series, 1170*, 0–6. doi:10.1088/1742-6596/1170/1/012056
28. Yousefi I., Pakravan M., Rahimi H., Bahador A., Farshadzadeh Z., Haririan I. (2017): An investigation of electrospun Henna leaves extract-loaded chitosan based nanofibrous mats for skin tissue engineering. *Material Science Engineering C, 75*, 433–444. doi:10.1016/j.msec.2017.02.076
29. Rahim A., Garba Z. (2015): Optimization of preparation conditions for activated carbon from Prosopis africana seed hulls using response surface methodology. *Desalination*

and Water Treatment, 57, 1–10. doi:10.1080/19443994.2015.1086695

30. Scaffaro R., Lopresti F., Botta L. (2017): Preparation, characterization and hydrolytic degradation of PLA/PCL co-mingled nanofibrous mats prepared via dual-jet electrospinning. *European Polymer Journal, 96*, 266 277. doi:10.1016/j.eurpolymj.2017.09.016
31. El-Sayed S., Mahmoud K.H., Fatah A.A., Hassen A. (2011): DSC, TGA and dielectric properties of carboxymethyl cellulose/polyvinyl alcohol blends. P*hysica B: Condensed Matter, 406*, 4068–4076. doi:10.1016/j.physb.2011.07.050
32. Kaya M., Khadem S., Cakmak Y.S., Mujtaba M., Ilk S., Akyuz L., Salaberria A.M., Labidi J., Abdulqadir A.H., Deligöz E. (2018): Antioxidative and antimicrobial edible chitosan films blended with stem, leaf and seed extracts of Pistacia terebinthus for active food packaging. *RSC Advances, 8*, 3941–3950. doi:10.1039/c7ra12070b
33. Zhang J., Wang S., Zhao D., Zhang Y., Pang W., Zhang B., Li Q. (2017): Improved processability and performance of biomedical devices with poly(lactic acid)/poly(ethylene glycol) blends. *Journal of Applied Polymer Science, 134*, 45194. doi:10.1002/app.45194
34. Chieng B.W., Ibrahim N.A., Yunus W.M.Z.W., Hussein M.Z. (2013): Plasticized poly(lactic acid) with low molecular weight poly(ethylene glycol): Mechanical, thermal, and morphology properties. *Journal of Applied Polymer Science, 130*, 4576–4580. doi:10.1002/app.39742
35. Vaes D., Van Puyvelde P. (2021): Semi-crystalline feedstock for filament-based 3D printing of polymers. *Progress in Polymer Science, 118,* 101411. doi:10.1016/j.progpolymsci.2021.101411
36. Cesur S., Ilhan E., Tut T.A., Kaya,E. Dalbayrak B., Bosgelmez-Tinaz G., Arısan E.D., Gunduz O., Kijeńska-Gawrońska E. (2023): Design of Cinnamaldehyde- and Gentamicin-Loaded Double-Layer Corneal Nanofiber Patches with Antibiofilm and Antimicrobial Effects. *ACS Omega, 8*, 28109–28121. doi:10.1021/acsomega.3c00914
37. Almasian A., Najafi F., Eftekhari M., Ardekani M.R.S., Sharifzadeh M., Khanavi M., (2020): Polyurethane/carboxymethylcellulose nanofibers containing Malva sylvestris extract for healing diabetic wounds: Preparation, characterization, in vitro and in vivo studies. *Materials Science Engineering C, 114*, 111039. doi:10.1016/j.msec.2020.111039
38. Al-Kaabi W.J., Albukhaty S., Al-Fartosy A.J.M., Al-Karagoly H.K., Al-Musawi S., Sulaiman G.M., Dewir Y.H., Alwahibi M.S., Soliman D.A. (2021): Development of Inula graveolens (L.) Plant Extract Electrospun/Polycaprolactone Nanofibers: A Novel Material for Biomedical Application. *Applied Sciences, 11*. doi:10.3390/app11020828
39. Sriyanti I., Edikresnha D., Rahma A., Munir M.M., Rachmawati H., Khairurrijal K. (2017): Correlation between Structures and Antioxidant Activities of Polyvinylpyrrolidone/Garcinia mangostana L. Extract Composite Nanofiber Mats Prepared Using Electrospinning. *Journal of Nanomaterials, 2017*, 9687896. doi:10.1155/2017/9687896
40. Merghoub N., El Btaouri H., Benbacer L., Gmouh S., Trentesaux C., Brassart B., Terryn C., Attaleb M., Madoulet C., Benjouad A., Amzazi S., El Mzibri M., Morjani H. (2016): Inula Viscosa Extracts Induces Telomere Shortening and Apoptosis in Cancer Cells and Overcome Drug Resistance. *Nutrition and Cancer, 68*, 131–143. doi:10.1080/01635581.2016.1115105
41. Rechek H., Haouat A., Hamaidia K., Pinto D.C.G.A., Boudiar T., Válega M.S.G.A., Pereira D.M., Pereira R.B., Silva A.M.S. Inula viscosa (L.) (2023): Aiton Ethanolic Extract Inhibits the Growth of Human AGS and A549 Cancer Cell Lines. *Chemistry & Biodiversity, 20*, e202200890. doi:10.1002/cbdv.202200890